Regular article

Characterizing the effects of in-situ sensitization on stress corrosion cracking of austenitic steels in supercritical water

Kai Chen, Jiamei Wang, Donghai Du *, Xianglong Guo, Lefu Zhang *

School of Nuclear Science and Engineering, Shanghai Jiao Tong University, Dongchuan Road, Shanghai 200240, PR China

ABSTRACT

This work compared the stress corrosion cracking (SCC) susceptibility of two austenitic alloys in supercritical water (SCW), and revealed the quantitative difference of SCC growth rates through scanning transmission electron microscopy (STEM). Results showed that in-situ sensitization and creep occurred on the specimens during the SCC tests in SCW environment. Higher degree of Cr-depletion at the grain boundary ahead of the SCC crack tip was identified in the Fe-^{25}Cr steel specimen, which has suffered severer in-situ sensitization because of the lower Cr content than the Ni-$^{29.3}$Cr alloy specimen, and this in turn increased the creep susceptibility.

© 2018 Acta Materialia Inc. Published by Elsevier Ltd. All rights reserved.

310S stainless steel (SS) and Alloy 690 are modified austenitic alloys with higher chromium (Cr) content than 304/316 SS and Alloy 600 to increase the corrosion resistance and high temperature mechanical properties, and both materials are among the most promising structural materials for the generation IV supercritical water (SCW) reactors [1–3]. Laboratory results have confirmed that austenitic steels exhibited some susceptibility to stress corrosion cracking (SCC) in SCW over the temperature ranging from 400 to 650 °C [4–16]. However, the published data showed contradictory results when comparing the SCC susceptibilities of SS and nickel alloys in SCW. To date, investigations have focused mainly on the SCC initiation behavior in SCW by conducting slow strain rate tensile (SSRT) tests with an inherent accelerating effect on the SCC behavior [4–14], thus the relevance of the accelerated results to the field conditions remains unclear. SCC growth behavior in SCW shows much higher relevance and represents the failure through the whole microstructure of the thick components. Unfortunately, this kind of work is rarely found. The aim of our work is to clarify the difference of SCC susceptibility between 310S SS and Alloy 690 in SCW through microstructural characterization. The crack tip morphology and element distribution were characterized to evaluate the contribution of creep and in-situ sensitization on the SCC growth rate.

The materials were type 310S SS and Alloy 690 in solution annealed and mill annealed conditions, respectively. Both materials are modified alloys with higher Cr content, as listed in Table 1. Standard compact tension specimens with 12.7 mm thickness and 5% side grooves were used for the SCC tests. The SCC tests were conducted in SCW environment at

550 °C. The water in the reservoir column was deaerated by argon to create a low corrosion potential environment, and the pressure was maintained at 25 MPa with a water flow rate of 1 L/h. The crack length of the specimen was continuously monitored in-situ via the reversed direct current potential drop method [17]. During the SCC tests, constant stress intensity factor (K) of 25 MPa√m was maintained to measure the SCC crack growth rate (CGR). Detailed description of the SCC tests could be found in our recent publications [15–17].

The specimens were micro-characterized prior to and after the SCC tests using complementary microstructural analysis techniques. More specifically, an FEI field emission scanning electron microscopy (FE-SEM) (NOVA NanoSEM 230) was used to characterize the crack tips after the tests. An TESCAN FE-SEM (GAIA3 GMU Model 2016) equipped with DualBeam focused ion beam (FIB) was used to prepare cross-section transmission electron microscopy (TEM) coupons at the intergranular (IG) crack tips, and then extracted from the coupons using TEM lift-out technique and thinned using the FIB to about 100 nm. The following TEM characterization on the FIB specimens was performed on an FEI Talos F200X TEM operated at 200 kV and equipped with four Bruker silicon drift detectors (SSD) for energy dispersive X-ray (EDX) imaging analysis. The scanning TEM (STEM) EDX "line scanning" and "mapping" were performed to evaluate the element distribution and oxidation at the crack tips.

The SCC CGR of the 310S SS specimen in 550 °C SCW was 1.4 × 10^{-7} mm/s, ~17 times higher than the Alloy 690 specimen (8.3 × 10^{-9} mm/s) as listed in Table 1. Detailed crack growth response curves could be found in our recent work [16,18]. The long testing times, >3000 h for both specimens, raise the concern of sensitization during the high-temperature tests. Thus, the degree of sensitization

* Corresponding authors.
E-mail addresses: 0703ddh@sjtu.edu.cn (D. Du), lfzhang@sjtu.edu.cn (L. Zhang).

Table 1
Comparison of the chemical composition, SCC CGR, test duration and DOS of the two materials.

Specimen	Chemical composition (wt%)	CGR (mm/s)	Test duration	DOS (prior)	DOS (after)
310S SS	25.01%Cr, 19.98%Ni, 0.050%C, Fe balance	1.4×10^{-7}	3681 h	10.7%	33.0%
Alloy 690	29.30%Cr, 9.21%Fe, 0.034%C, Ni balance	8.3×10^{-9}	3002 h	0%	1.9%

(DOS) was measured on the as-received and exposed samples using double loop electrochemical potentiokenetic reactivation (DL-EPR) method [19], and the results are also listed in Table 1. The DOS of 310S SS prior to the SCC test was 10.7%, and increased dramatically to 33.0% after the SCC test, suggesting that severe sensitization occurred during the test. In contrast, the as-received Alloy 690 showed no sensitization, and suffered only a small DOS of 1.9% after the SCC test. To understand the development of different DOS values and their effects on the SCC growth behavior of 310S SS and Alloy 690, detailed microstructural characterization was performed at the active crack tips for both specimens.

Fig. 1 shows SEM and TEM images of the SCC crack tip in the 310S SS specimen. IG creep cracks lack of oxidation with cavity-like features were identified near the SCC crack tip (Fig. 1a), suggesting possible contribution of creep to the whole crack growth. The TEM HAADF image revealed the presence of semi-continuous carbides along the grain boundary (GB) just ahead of the crack tip (Fig. 1b). Selective area diffraction (SAD) confirmed that the IG carbides were face centered cubic (fcc) semi-coherent $M_{23}C_6$. Further STEM-EDX mapping analysis (Fig.1c–e) showed severe Cr-depletion zone with Fe and Ni-enrichment at the GB ahead of the crack tip. Since the EDX elemental maps are qualitative results, STEM-EDX spectrum line scanning (Fig. 1f) was conducted to quantitatively reveal a minimum Cr content of ~5.8% at the Cr-depletion zone, compared to the bulk Cr content of 25.01% in 310S SS. This highly Cr-depletion zone at the GB seems to be the result of in-situ sensitization, and is in good agreement with the high DOS value (33%) of the exposed 310S SS sample, which might be responsible for the high SCC CGR of 310S SS specimen.

Fig. 2 shows the similar characterization of the SCC crack tip in the Alloy 690 specimen. The HADDF image (Fig. 2b) showed the SCC crack tip with a diameter of ~500 nm. Further STEM-EDX mapping and line scanning analysis (Fig. 2c–d) revealed similar Cr-depletion zone with Fe and Ni-enrichment at the GB ahead of the crack tip. The minimum Cr content was ~18% comparing to the bulk Cr content of 29.30% in Alloy 690 (Fig. 2f). This moderate Cr-depletion was in good agreement with the small DOS value (1.9%) of the exposed Alloy 690 sample. Comparing the EPR and STEM-EDX results, the sensitization and Cr-depletion at the GBs of the 310S SS specimen is much severer than the Alloy 690 specimen, which accounts well with the SCC susceptibilities of these two specimens.

The increased GB Cr-depletion or sensitization near the crack tips during the SCC tests might be caused by two potential contributors. The first one is might be the oxidation on the crack walls at the crack tip where Cr was consumed to form Cr-rich oxide film. Then Cr at the GBs ahead of the crack tip was driven by a Cr concentration gradient, and tended to diffuse to the crack tip to form oxide because Cr diffuses faster along GBs than in matrix. Noting that the oxidation induced Cr-depletion ahead of the crack tip always accompanies with Fe-depletion at the same region due to the preferential oxidation of Cr and Fe [20]. However, the Cr-depletion region in this study (Figs. 1 and 2) is Fe-rich and Ni-rich, which is obviously not a result of oxidation induced atom diffusion and enrichment. Thus, the Cr-depletion ahead of the crack tip was caused by another contribution, the in-situ sensitization during the SCC tests. To further confirm this hypothesis, SEM and STEM-EDX were conducted on the GBs far away from the crack tips of the samples prior to and after the SCC tests, as shown in Fig. 3. Firstly, for the 310S SS specimen, the GB carbide coverage increased from 15% to 59% after the SCC test (Fig. 3a and b), indicating the formation of GB carbides during in-situ sensitization. Furthermore, the line scanning results at the GB of the exposed base metal (Fig. 3d) showed similar depth of Cr-depletion comparing with the crack tip in Fig. 1. Although the IG carbide density of the Alloy 690 specimen showed little change after the SCC test (Fig. 3e and f), moderate Cr depleted zone with minimum Cr content of 19% was identified by STEM-EDX line scanning, as shown in Fig. 3h. Since the GBs in Fig. 3 was characterized far away from the crack tip in the exposed samples and there was no oxidation occurred in these GBs, the observed IG Cr-depletion in 310S SS and
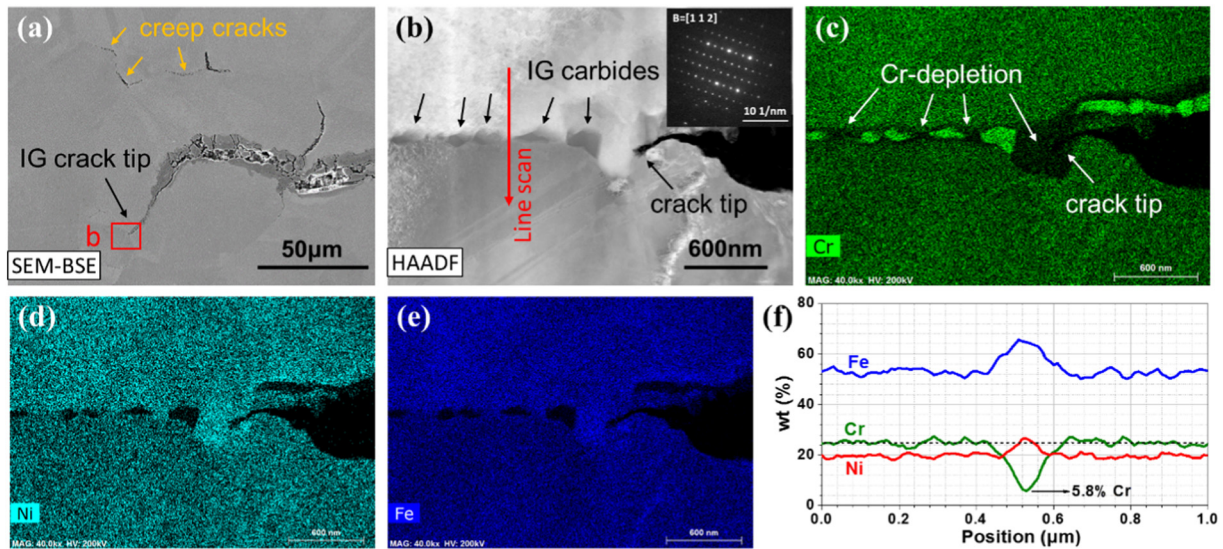

Fig. 1. Characterization of the SCC crack tip in 310S specimen, (a) SEM image of the SCC crack tip with creep features, (b) HAADF STEM image at the SCC crack tip showing the presence of IG carbides, which were identified via electron diffraction as $M_{23}C_6$ (inserted in Figure b), (c–e) STEM-EDX spectrum images showing the Cr-rich $M_{23}C_6$ carbides and the extent of Cr-depletion, (f) STEM-EDX spectrum lines showing the depth and width of Cr-depletion at the crack tip.